Application of Dynamic Centrifugal Compressor Model for Mechanical Vapor Recompression System Simulation

Le Wang
Hefei General Machinery Research Institute, China, People's Republic of, wangle4127@gmail.com

Guangbin Liu
State key laboratory for compressor technology, Hefei General Machinery Research Institute, People's Republic of China, guangbin0805@163.com

Chuandong Xie
State Key Laboratory of Compressor Technology, Hefei General Machiney Research Institude, People's Republic of China, 853997022@qq.com

Jun Xiao
Hefei General Machinery Research Institute, China, People's Republic of, xjcompressor@163.com

Chenyan Zhang
Hefei General Machinery Research Institute, China, People's Republic of, zcy.hf@163.com

Application of Dynamic Centrifugal Compressor Model for Mechanical Vapor Recompression System Simulation

Wang Le[1]*, Liu Guangbin[2], Xie Chuandong[1], Xiao Jun[1], Zhang Chenyan[1]

[1] State Key Laboratory of Compressor Technology, Hefei General Machinery Research Institute Co., Ltd., Hefei, Anhui Province, P. R. China
E-mail address: wangle4127@gmail.com

[2]College of Mechanical and Electronic Engineering, Qingdao University of Science and Technology, Qingdao, Shandong Province, P. R. China

* Corresponding Author

ABSTRACT

The construction of the centrifugal compressor model and its application for the mechanical vapor recompression (MVR) system dynamic simulation were presented. Instead of lumped loss equations, the centrifugal compressor model used established one-dimensional (1D) loss equations found in open literature. The losses were modeled not only in the impeller but also in the diffuser and the volute. Given specified geometry, rotational speed and suction condition, the model was capable of calculating the static and total temperatures, velocities, static and total pressures, pressure losses, polytropic head and isentropic efficiencies for each compressor component. The behavior of the centrifugal compressor of the MVR system was investigated by both the model and the experiments. The model was helpful for the designer to minimize the magnitude of the losses and justify optimum design decisions. The performance and the surge curve over the entire operating conditions provided by the model were incorporated with the MVR system dynamic simulation and then it was possible for dynamic study on the response of the anti-surge control under the situation of the check valve failure.

1. INTRODUCTION

Analytical method of performance prediction which is able of predicting the overall dimensions and performance curve of the stage plays an important role in designing a centrifugal compressor, because it can be used to perform parametric studies to demonstrate the influence of changes in geometry on the performance under both design and off-design conditions. Although CFD methods has been improved recently, 1D models still play important roles for predicting centrifugal compressor performance due to its accuracy and low computational cost.
To develop a proper numerical model, losses encountered in compressors must be appropriately dealt with. The origin and effects of loss mechanism were discussed in details (Fabio B, 2011 and Oh, H. W. et.al. 1997). Losses in centrifugal compressors are commonly classified as incidence loss, friction loss, clearance loss, backward loss and volute loss (Barend W. et. al., 2005, Wei J. et. al. 2006, and Bing H. et. al. 2012). The capability and limitation of the exist models for predicting incidence loss was reported (Helen M., 2006). Based on thermodynamic principles, various loss models mentioned will be employed in this one dimensional compressor model to simulate compressor presentation by calculating individual component performances based on various measurable parameters.

In order to reducing energy costs and CO2 foot-print, mechanical vapor recompression system (MVR) is used for thermal separation processes such as evaporation and distillation are energy intensive instead of multiple-effect evaporation system. For medium and high capacities, centrifugal compressor (fan) is the most commonly used type for gas compression with a limited operational range and control of the compressors is crucial for safe and efficient operation.

2. COMPRESSOR MODEL

2.1 Compressor Structure

The centrifugal compressor is composed of four components, as shown in Figure. 1. 1 and 2 are the impeller inlet and outlet and 2 is also the diffuser inlet. 3 are the vaneless diffuser outlet and vaned diffuser inlet. 4 is the vaned diffuser outlet and volute inlet and ~~6~~ 5 is the volute outlet.

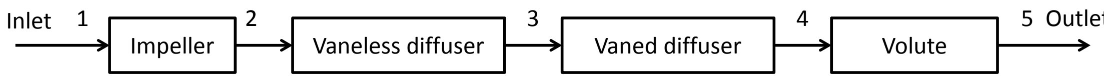

Figure 1: Compressor flowing components

For each component of compressor, the variables which are the inlet pressure, inlet temperature, inlet velocities, outlet pressure, outlet temperature and outlet velocities were used to fully describe it. A set of algebraic equations which relate the inlet and outlet variable were developed from the moment of momentum equation, steady flow energy equation, mass continuity equation, thermodynamic equation of state, and trigonometric relations from corresponding velocity vector diagrams at the mean stream line. The non-dimensional losses of the components are computed as functions of the geometry, velocity, temperature, and pressure.

2.2 Impeller Model

The impeller is the only rotating component in the compressor so the losses of impeller are converted into a total relative pressure loss described as (Aungier, 1995):

$$\Delta p_{tr} = f_c(p_{tr1} - p_1)\sum_i \eta_i \tag{1}$$

where p_{tr1} and p_1 are the total relative pressure and static pressure at impeller ~~exit~~ inlet respectively, f_c is a correction factor and can be calculated as

$$f_c = \frac{\rho_{tr2} T_{tr2}}{\rho_{tr1} T_{tr1}} \tag{2}$$

where ρ_{tr} is the total relative density. The actual total relative pressure at the impeller exit is defined as

$$\Delta p_{tr2,actual} = \Delta p_{tr2,ideal} - \Delta p_{tr} \tag{3}$$

where $p_{tr2,ideal}$ can be calculated as

$$\Delta p_{tr2,ideal} = p_{2,ideal}\left[1 + \left(\frac{\kappa - 1}{2}\right) Ma_{r2}^2\right]^{\frac{\kappa}{\kappa-1}} \tag{4}$$

In the 1D losses model, there are commonly 9 losses that could affect the performance of the impeller, which will be discussed as follows.

Table 1: A set of loss models for impeller

Loss mechanism	Loss model	Description	Reference

Shock loss	$\eta_{sh} = 1 - \left(\frac{W_{Th}}{W_1}\right)^2 - \frac{2}{(\kappa-1)Ma_{r1}^2}\left[(\frac{p_{Th}}{p_1})^{\frac{\kappa-1}{\kappa}} - 1\right]$ $W_{Th} = \frac{C_{rTh}}{\sin\beta_{Th}}$	W_{Th}: the impeller throat relative velocity C_{rTh}: the throat radial velocity β_{Th}: the relative blade angle at the throat	Whitfield and Baines, 1990
Incidence loss	$\eta_{inc} = 0.8\left[1-\frac{C_{r1}}{W_1\sin\theta_{m1}}\right]^2 + \left[\frac{t_{b1}Z}{2\pi r_1\sin\theta_{m1}}\right]^2$	t_{b1}: the impeller inlet blade thickness θ_{m1}: the inlet mean blade angle	Aungier, 1995
Clearance loss	$\eta_{cl} = \frac{2\dot{m}_{cl}\Delta p_{cl}}{\dot{m}\rho_1 W_1^2}$	Δp_{cl}: the pressure difference across the gap $\dot{m}_{cl}$: the clearance gap leakage flow rate	Aungier, 1995
Skin friction loss	$\eta_{sk} = 4C_f\left(\frac{\bar{W}}{W_1}\right)^2\frac{L_B}{D_H}$ $\bar{W}^2 = \frac{W_1^2+W_2^2}{2}$	L_B: the blade mean camberline length D_H: the hydraulic diameter	Aungier, 1995
Blade loading loss	$\eta_{bl} = \frac{(\Delta W/W_1)^2}{24}$	ΔW: the average blade velocity difference	Thanapandi and Prasad, 1990
Hub to shroud loading loss	$\eta_{hs} = \frac{(\bar{k}_m\bar{b}\bar{W}/W_1)^2}{6}$	$\bar{W}$: average relative velocity $\bar{k}_m$: the passage curvature $\bar{b}$: the average width.	Oh *et al*. 1997
Blockage loss	$\eta_{blo} = \left[\frac{(\lambda-1)C_{r2}}{W_1}\right]^2$	λ: the tip distortion factor	Oh *et al*. 1997
Mixing loss	$\eta_{mix} = \left[\frac{C_{r,wake}-C_{r,mix}}{W_1}\right]^2$	$C_{r,\ wake}$: the radial velocity of the wake $C_{r,\ mix}$: the radial velocity of the mixed flow.	Aungier, 1995
Supercritical Mach number loss	$\eta_{scma} = 0.4\left[\frac{(Ma_{r1}-Ma_{cr})W_{max}}{W_1}\right]^2$	Ma_{cr}: the inlet critical Mach number	Aungier, 1995

2.3 Vaneless Diffuser Model

The total pressure loss conversion can be mathematically described as

$$\Delta p_{t3} = f_c(p_{t2} - p_2)\sum_i \eta_i \tag{5}$$

The flow conditions are the same at both the inlet of the exit of the impeller and the vaneless diffuser.

Table 2: A set of loss models for vaneless diffuser

Loss mechanism	Loss model	Description	Reference
Skin friction loss	$\eta_{sk} = 4C_f\left(\frac{\bar{C}}{C_2}\right)^2\frac{r_3-r_2}{D_h}$ $\bar{C} = \frac{C_2^2+C_3^2}{2}$	D_h: the hydraulic diameter C_f: the skin friction coefficient	Aungier, 1995
Diffusion loss	$\eta_{df} = -2(1-E)(\frac{C_{3,id}-C_2}{\rho_2 C_2})$	E: the diffusion efficiency	Johnston and Dean, 1966

The actual total pressure is the difference of the ideal total pressure and the total pressure loss. The actual total pressure is used to calculate the other actual exit conditions of the vaneless diffuser using the velocity diagrams, total temperature relationship to calculate the static temperature, the total pressure relationship to calculate the static pressure, the density, and the assumption that the total temperature is constant due to constant enthalpy. The actual exit conditions can be used to determine the component mean thermodynamic efficiency and power consumption parameters.

2.4 Vaned Diffuser Model

Similar to the vaneless diffuser, the non-dimensional loss parameter for the vaned diffuser is converted into a total pressure loss. The total pressure loss conversion can be mathematically described as

$$\Delta p_{t4} = f_c(p_{t3} - p_3)\sum_i \eta_i \tag{6}$$

The loss parameters are calculated using the inlet, throat, and isentropic exit conditions. The inlet conditions are equal to the actual exit conditions of the vaneless diffuser.

Table 3: A set of loss models for vaned diffuser

Loss mechanism	Loss model	Description	Reference
Skin friction loss	$\eta_{sk} = 4C_f\left(\frac{\bar{C}}{C_3}\right)^2 \frac{L_B/D_H}{(2\delta/D_H)^{0.25}}$ $\frac{2\delta}{D_H} = \frac{5.142C_f L_B}{D_H}$	$\frac{2\delta}{D_H}$: the boundary layer approximation	Aungier, 1995
Incidence loss	$\eta_{inc} = 0.8\left(\frac{C_3 - C_3^*}{C_3}\right)^2, C_3 \le C_{3s}$ $\eta_{inc} = 0.8\left[\left[\left(\frac{C_3}{C_{3s}}\right)^2 - 1\right]\left(\frac{C_{Th}}{C}\right)^2 + \left(\frac{C_{3s} - C_3^*}{C_{3s}}\right)^2\right]^2$ $, C_3 > C_{3s}$	C_{3s}: the absolute stall velocity C^*_3: the velocity at the optimum incidence angle.	Aungier, 1995
Blockage loss	$\eta_{blo} = \left[\frac{(\lambda - 1)C_{r4}}{C_4}\right]^2$	λ: the tip distortion factor	Oh *et al*. 1997
Wake mixing loss	$\eta_{mix} = \left[\frac{C_{r,wake} - C_{r,mix}}{C_3}\right]^2$	$C_{r,\ wake}$: the radial velocity of the wake $C_{r,\ mix}$: the radial velocity of the mixed flow.	Aungier, 1995

Similar as the impeller, the actual total pressure is the difference of the ideal total pressure and the total pressure loss.

2.5 Volute Model

The non-dimensional loss parameter for the vaned diffuser is converted into a total pressure loss. The total pressure loss conversion can be mathematically described as

$$\Delta p_{t4} = f_c(p_{t3} - p_3)\sum_i \eta_i \tag{7}$$

The inlet conditions of the volute are equal to the exit conditions of the actual vaned diffuser.
There are three losses described in the volute.

Table 4: A set of loss models for volute

Loss mechanism	Loss model	Description	Reference
Meridional velocity loss	$\eta_{mv} = \left(\frac{C_{4r}}{C_4}\right)^2$		Weber and Koronowski, 1986

Tangential velocity loss	$\eta_{tv}=\frac{1}{2}\frac{r_4C_{4u}^2}{r_5C_4^2}\left(1-\frac{1}{SP^2}\right), SP\geq 1$ $\eta_{tv}=\frac{r_4C_{4u}^2}{r_5C_4^2}\left(1-\frac{1}{SP^2}\right), SP<1$	SP: the volute sizing parameter	Weber and Koronowski, 1986
Skin friction loss	$\eta_{sk}=4C_f\left(\frac{C_5}{C_4}\right)^2\frac{L}{D_h}$	L: the mean stream line path length of volute D_h: the hydraulic diameter of volute	Aungier, 1995

Similar as the impeller, the actual total pressure is the difference of the ideal total pressure and the total pressure loss.

2.6 Performance Maps

A performance map describes how a compressor’s polytropic head and efficiency vary with volumetric suction flowrate and rotational speed for a specific set of suction conditions (i.e., fluid molecular weight, pressure, temperature, compressibility, and isentropic exponent at the inlet of the compressor). The compressor characteristics are represented in terms of component maps. The compressor model aims to plot a component map so as to better support simulation process.

3. MECHANICAL VAPOR RECOMPRESSION

3.1 MVR System

MVR system works like an “open heat-pump” (Carnot process), where the vapors are recompressed up to the pressure level of the heating steam. The driving energy for the evaporation process results from the isentropic enthalphy increase of the vapor steam. The vapor condensate and the purge stream as well are used to preheat the feed nearly to the operation temperature of the unit. Due to this intensive heat recovery the make-up steam consumption is nearly zero, only for the start up a small heat quantity is required. A typical MVR system configuration of the capacity 1000kg h^{-1} for waste-water treatment is shown in Figure 1. Feed waste-water enters the heat exchange and is heated to the temperature of 70 ℃ by cooling the condensed water from the film evaporator. It flows into the film evaporator and is evaporated to the vapor of the pressure 31.2kPa (saturation pressure of 70℃), meanwhile the discharge vapor from the compressor is cooled to the saturated mixture which will be separated by the separator. The vapor fraction from the separator is suctioned by the compressor and compressed to the pressure of 47.4kPa (saturation pressure of 80℃), while the liquid fraction is circulated to the file evaporator by the pump.

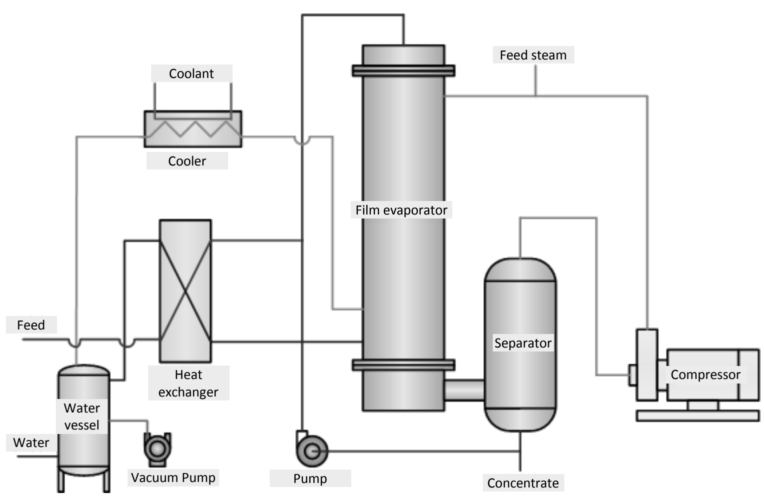

Figure 1: MVR system

3.2 Process control and anti-surge control

Process control is used to adjust variables, such as valve opening, temperature and pressure, in order to ensure stable performance of a dynamic process. This is done by having a controller which can adjust an input to the system. The physical equations that govern the controller are originated from the compressor performance map. The application of the process control for safety is the anti-surge control for the centrifugal compressor. The main goal of the anti-surge control is to prevent the compressor from surging. This is done by having a recycle valve at the compressor outlet pipe that allows flow back to the inlet. The set point of the controller is set to have a specified distance to the surge line of the compressor called the surge margin. The definition of the surge margin varies between different controllers but the idea is to set a value at an appropriate distance from the surge line in order to have a safety margin for the controller. PID is normally used due to the high requirement of fast and accurate controller. The business chemical process simulation software provides a useful tool to investigate the dynamic behavior of the centrifugal compressor when the anti-surge control is activated.

4. RESULTS AND DISSCUSSION

4.1 Validation of Compressor Model

The prototype compressor of the MVR system was developed under the design condition of the inlet temperature 70℃, the inlet static pressure 31.2kPa and the rotating speed 20000rpm. Its geometry data is shown in Table ~~4~~. 5

Table 5: Geometry data of compressor

Parameter	**Value**	**Parameter**	**Value**
Impeller inlet tip diameter /mm	166.80	Impeller outlet blade angle /°	60
Impeller inlet hub diameter /mm	80.12	Vaned diffuser inlet diameter /mm	381.60
Impeller inlet blade thickness /mm	3.00	Vaned diffuser outlet diameter /mm	480.20
Impeller blade inlet angle /°	40	Vaned diffuser outlet Blade Angle /°	39.23
Impeller blade number	16	Vane number	13

The proposed model was validated against experimental results according to the compressor. As illustrated in Figure 2, the pressure ratios predicted by the model had good agreement with the values measured by the experiment for the rotating speed of 18500rpm and 20000rpm respectively.

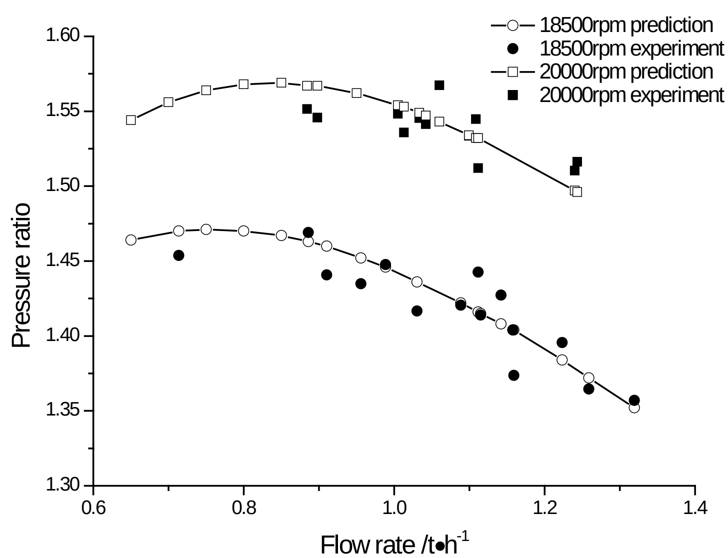

Figure 2: Comparison of predicted and experimental compressor pressure ration

The performance maps of the centrifugal compressor for the MVR System were plotted as well as the compressor surge line in Figure 3. The surge point is dependent on multiple parameters and hardly predicted precisely by the model, so the flow of the max pressure ratio is assumed empirically to be the surge flow.

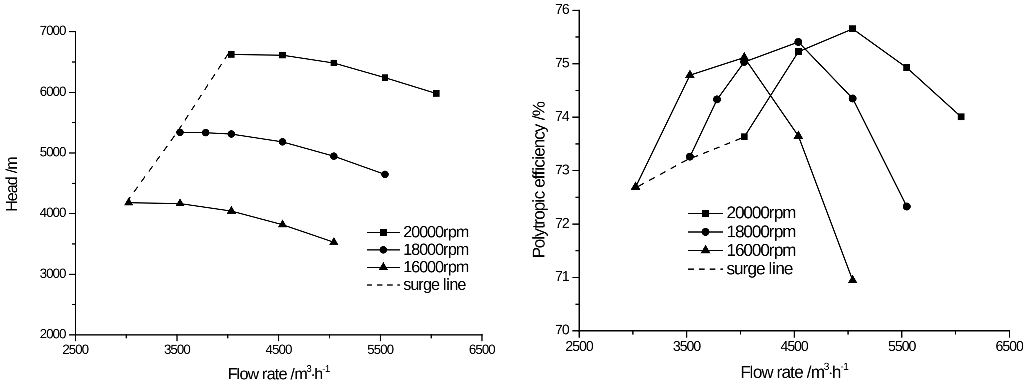

(a) Head vs. flow rate (b) Polytropic efficiency vs. flow rate

Figure 3: Performance maps of the centrifugal compressor

The situation of the check valve failure was chosen to predict the performance for the anti-control by the compressor surge module of HYSY. The rotation speed was kept at 17500rpm. The control line was set to 15% margin from the surge line. As shown in Figure 3, the trail of the compressor was moving towards the surge line. At the time of 66s, the anti-surge control took effect and made the anti-surge valve actuator positon to 44%. Then the flow was recycled to the compressor suction. At the time of 82s, the centrifugal compressor stayed again under the steady condition of the suction flow of 3868 $kmol \cdot h^{-1}$ and the discharge pressure of 251kPa as illustrated in Figure 5.

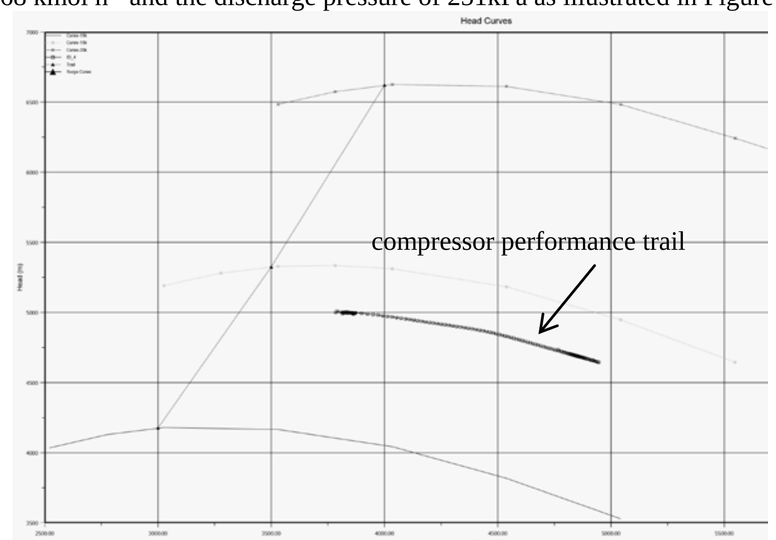

Figure 4: Compressor curve profile

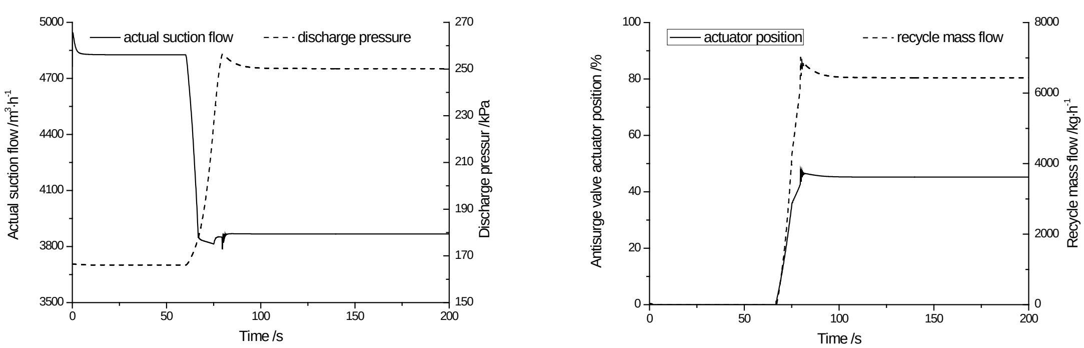

(a) compressor performance vs time (b) anti-surge valve performance vs time

Figure 5: Anti-surge control dynamical performance

6. CONCLUSIONS

In this paper, One-dimensional (1D) compressor model based on the thermodynamics has been constructed for the analysis of compressor performance. This model investigated the effect of each loss on the compressor performance. The model was verified by the experiment. Entire operating conditions provided by the model were used for the MVR system dynamic simulation and the dynamic study on the response of the response of the anti-surge control was done under the condition of the check valve failure.

NOMENCLATURE

The nomenclature should be located at the end of the text using the following format:

A	Reference flow area	r	Radius
b	Width	T	Static Temperature
C	Fluid absolute velocity	p	Static Pressure
D	Diameter	ρ	Density
Ma	Mach numbler	U	Tangential velocity
W	Relative velocity	α	Absolute flow angle
β	Relative flow angle	κ	Ratio of specific heats
PR	Pressure ratio	h	Specific enthalpy

Subscript

h	Hub	t	Tip
th	Throad		

REFERENCES

Aungier, R. H. (1995). Mean streamline aerodynamic performance analysis of centrifugal compressors. *Journal of Turbomachinery*, 117(3), 360-366.

Oh, H. W., Yoon, E. S., & Chung, M. K. (1997). An optimum set of loss models for performance prediction of centrifugal compressors. *Proceedings of the Institution of Mechanical Engineers, Part A: Journal of Power and Energy*, 211 A4(4), 331.

Thanapandi, P., & Prasad, R. (1990). Performance prediction and loss analysis of low specific speed submersible pumps. *Proceedings of the Institution of Mechanical Engineers, Part A: Journal of Power and Energy*, 204(4), 243-252.

Fabio B, Vincenzo D, (2011). 1D Simulation and Experimental Analysis of a Turbocharger Compressor for Automotive Engines under Unsteady Flow Conditions, *SAE Technical Paper*, 2011-01-1147

Barend W, Adriaan M, (2005). Determining the Impact of the different Losses on Centrifugal Compressor Design, *R&D Journal*, 21(3), 23-31.

Wei J, Jamil K, Roger A, (2006). Dynamic centrifugal compressor model for system simulation, *Journal of Power Sources*, 158, 1333–1343.

Barend W, Adriaan M, (2005).Determining the Impact of the different Losses on Centrifugal Compressor Design, *R&D Journal*, 21(3), 23-31.

Wei J, Jamil K, Roger A, (2006). Dynamic centrifugal compressor model for system simulation. *Journal of Power Sources*, 158, 1333–1343.

Bing H, Tan L, Cao S and Lu L, Prediction method of impeller performance and analysis of loss mechanism for mixed-flow pump, Science China Technological Sciences, Vol.55 No.7: 1988–1998, 2012.

Helen M, (2006). Development of A 1-D Performance Prediction Technique for Automotive Centrifugal Compressor. *PhD Thesis*, Loughborough University.

ACKNOWLEDGEMENT

This work was supported in part by the National Key Research and Development Program of China (No. 2016YFF0203300) and the National Natural Science Foundation of China (No. 51606058).